Available online at www.sciencedirect.com
ScienceDirect
Journal of Sound and Vibration 302 (2007) 167–177
JOURNAL OF SOUND AND VIBRATION
www.elsevier.com/locate/jsvi

The analysis of dynamic instability on the large amplitude vibrations of a beam with transverse magnetic fields and thermal loads

Guan-Yuan Wu*

Department of Fire Science, Central Police University, 56 Shu-jen Rd., Ta-kang, Kwei-san, Tao-yuan, 333 Taiwan, ROC

Received 13 February 2006; received in revised form 13 November 2006; accepted 19 November 2006
Available online 2 January 2007

Abstract

The dynamic instability of a pinned beam subjected to an alternating magnetic field and thermal load with the nonlinear strain, and made of physically nonlinear thermoelastic material has been studied. Applying the Hamilton's principle, the equation of motion with damping factor, induced current and thermal load is derived. Using the Galerkin's method, the governing equation is reduced to a time-dependent Mathieu equation. The incremental harmonic balance (IHB) method is applied to analyse the dynamic instability. The effects of non-dimensional parameters frequency ratio (Ω), load factor (φ), amplitude ($\|a\|$), damping factor (k_1) and temperature increment (ΔT) on the dynamic instability are obtained and discussed. Results show that the characteristics of magnetoelastic instability for the beam having the large deformation are distinctive from those of the beam having small deformation.

1. Introduction

The effects of magnetic forces on the stress, motion and stability of the solid body have been discussed by several studies. One of the complicated problems of magneto-solids mechanics is the treatment of the interaction of electromagnetic fields with deformable structures. In order to analyse these phenomena, several theoretical models and numerical programmes have been developed for studying the effect of magnetoelastic interactions on the mechanical behavior of ferromagnetic structures such as beams, strips, plates and shells [1–9]. The authors of these papers studied the magneto-solids mechanics arisen from a nonlinear interactions between the linear/nonlinear magnetization of structures and an applied magnetic field.

It is well known that temperature increase may cause a quite significant change in the dynamic behavior of a structure, as temperature fields introduce thermal stress due to thermal expansion or contraction, and cause buckling of structures with two fixed ends [10]. On the other hand, when the large amplitude vibration is considered, the dynamic instability of the system will be influenced by the nonlinear effect of large deformation [11]. Therefore, the problem of geometrically nonlinear vibration with magnetic field and thermal

*Tel.: 886 3 3185326; fax: 886 3 3282321.
E-mail address: una210@mail.cpu.edu.tw.

0022-460X/$ - see front matter © 2006 Elsevier Ltd. All rights reserved.
doi:10.1016/j.jsv.2006.11.012

load is an interesting one. In fact, the magnetic force and the temperature variation have an interactive effect on the magnetoelastic structures. Although, there is much research on modeling for the linear/nonlinear magnetization of structures, the work of variation of thermal load and large deformation on the dynamic instability of the structures has not been considered simultaneously. Recently, the mean of estimation of thermal effect in the magnetic field with the linear thermoelastic relation has been developed by Wu [12]. The effects of magnetic field and thermal load on the dynamic instability and transient vibrations were discussed.

The aim of this study is to obtain a theoretical model for a pinned beam subjected to an alternating magnetic field and thermal load with the nonlinear strain, and made of physically nonlinear thermoelastic material. The equation motion is derived by Hamilton's principle in which the damping coefficient, induced current and thermal load are also considered. Using the Galerkin's method, the governing equation is reduced to a time-dependent Mathieu equation. By using the incremental harmonic balance (IHB) method [13–15], the nonlinear differential equation is transformed into a set of linearized incremental algebraic equations in terms of Fourier coefficients, and solved by each incremental step. It is found that the results of instability carried out by the IHB method agreed well with the results of Moon and Pao [1] for a small deformation. The principal instability regions are shown in the parameter space of the excitation magnitude versus frequency ratio, the frequency ratio versus dimensionless amplitude.

2. Equation of motion

2.1. Statement of problem

Consider a beam of length L, thickness h, and width d which is pinned at its ends, as shown in Fig. 1. An alternating uniform transverse magnetic field $\mathbf{B}_0 = B_m \cos(\Omega \times t)\, j$ in the y-direction and a uniform temperature increment ΔT are applied to the beam so that the magnetic force causes a displacement (u, v) of the beam, where u and v are the longitudinal and transversal displacements, respectively. The mid-surface of the undeformed beam is located at the x–z plane. The beam is initially straight having uniform thickness and the material properties are assumed to be isotropic and homogeneous.

2.2. Hamilton's principle

The mathematical model of the elastic system can be obtained through the application of the integral of the Hamilton's principle, which assumes the following aspect:

$$\delta I_L = \int_{t_1}^{t_2} \delta(K + W - U)\mathrm{d}t + \int_{t_1}^{t_2} \delta W_c \mathrm{d}t = 0, \tag{1}$$

where K is the kinetic energy of the system, U is the potential energy, W is the work of externally applied force, and W_c is the work of nonconservative force.

In this study, the associated nonlinear strain takes the form

$$\varepsilon_{xx} = \frac{\partial u}{\partial x} + \frac{1}{2}\left(\frac{\partial v}{\partial x}\right)^2. \tag{2}$$

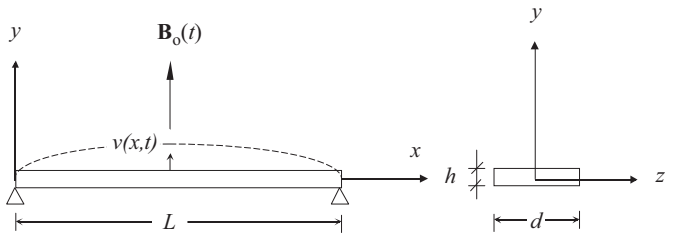

Fig. 1. The beam model.

The elastic strain energy caused by the increment ΔT and nonlinear strain has been expressed by the formulas [16]

$$U = \int_0^L \frac{EI}{2}\left(\frac{\partial^2 v}{\partial x^2}\right)^2 \mathrm{d}x + \int_0^L \frac{A}{2E}[E\varepsilon_{xx} - \gamma(T)]^2 \mathrm{d}x, \tag{3}$$

where E is the Young's modulus, I is the moment of inertia of the cross-section, A is the cross-section area, $\gamma(T)$ is the stress-temperature coefficient. In this study, the stress-temperature coefficient, $\gamma(T)$, is taken in the form [17],

$$\gamma(T) = E\alpha\Delta T + \hbar\alpha^2\Delta T^2 \tag{4}$$

where α is the coefficient of thermal expansion, and

$$\hbar = \hbar_1(1-2v) - 2\hbar_2(v^2-1) + \hbar_3 v^2. \tag{5}$$

In Eq. (5) $\hbar_1$, $\hbar_2$, $\hbar_3$ are Murnaghan's constants and v is Poisson's ratio. The terms of K and W assume the following aspect:

$$\begin{aligned}
K &= \frac{1}{2}\int_0^L m\left(\frac{\partial v}{\partial t}\right)^2 \mathrm{d}x,\\
W_T &= \int_0^L c\,\frac{\partial v}{\partial x}\,\mathrm{d}x,\\
W_P &= \int_0^L N(\mathrm{d}s - \mathrm{d}x) = \frac{1}{2}\int_0^L \left(\int_0^x p\,\mathrm{d}\xi\right)\left(\frac{\partial v}{\partial x}\right)^2 \mathrm{d}x,\\
\delta W_c &= \int_0^L c_d\left(\frac{\partial v}{\partial t}\right)\delta v\,\mathrm{d}x \quad \text{and}\\
W &= W_P + W_T,
\end{aligned} \tag{6}$$

where m is the mass of the beam per unit length, N is the axial compressive force of the beam, p is the body force of the beam per unit length, c is the body couple of the beam per unit length, and c_d is the damping ratio. Eq. (1) can be written as

$$\begin{aligned}
\delta I_L = \int_{t_1}^{t_2}\int_0^L \Bigg\{ & m\frac{\partial^2 v}{\partial t^2} + \frac{\partial c}{\partial x} + \frac{\partial}{\partial x}\left[\left(\int_0^x p\,\mathrm{d}\xi\right)\frac{\partial v}{\partial x}\right] + EI\,\frac{\partial^4 v}{\partial x^4}\\
& - EA\frac{\partial}{\partial x}\left\{\left[\frac{\partial u}{\partial x} + \frac{1}{2}\left(\frac{\partial v}{\partial x}\right)^2 - \frac{\gamma(T)}{E}\right]\frac{\partial v}{\partial x} + c_d\frac{\partial v}{\partial t}\right\}\delta v\,\mathrm{d}x\,\mathrm{d}t\\
& + \int_{t_1}^{t_2}\Bigg\{ EI\,\frac{\partial^2 v}{\partial x^2}\frac{\partial}{\partial x}(\delta v) - EI\,\frac{\partial^3 v}{\partial x^3}\delta v - c\delta v - \left(\int_0^x p\,\mathrm{d}\xi\right)\frac{\partial v}{\partial x}\,\delta v\\
& + EA\left[\frac{\partial u}{\partial x} + \frac{1}{2}\left(\frac{\partial v}{\partial x}\right)^2 - \frac{\gamma(T)}{E}\right]\frac{\partial v}{\partial x}\,\delta v\Bigg\}\Bigg|_0^L \mathrm{d}t\\
& - \int_{t_1}^{t_2}\int_0^L EA\frac{\partial}{\partial x}\left[\frac{\partial u}{\partial x} + \frac{1}{2}\left(\frac{\partial v}{\partial x}\right)^2 - \frac{\gamma(T)}{E}\right]\delta u\,\mathrm{d}x\,\mathrm{d}t\\
& + \int_{t_1}^{t_2} EA\left[\frac{\partial u}{\partial x} + \frac{1}{2}\left(\frac{\partial v}{\partial x}\right)^2 - \frac{\gamma(T)}{E}\right]\delta u\Bigg|_o^L \mathrm{d}t - \int_o^L \left(m\,\frac{\partial v}{\partial t}\delta v\right)\Bigg|_{t_1}^{t_2}\mathrm{d}x = 0.
\end{aligned} \tag{7}$$

For a pinned supported at both ends, the boundary conditions are

$$\begin{aligned}
&\delta u(0) = \delta u(L) = \delta v(0) = \delta v(L) = 0,\\
&v(0) = v(L) = 0, \text{ and } \partial^2 v/\partial x^2 = 0 \quad \text{at } x = 0 \text{ and } L.
\end{aligned} \tag{8}$$

The equilibrium equations can be obtained as

$$EA\frac{\partial}{\partial x}\left[\frac{\partial u}{\partial x}+\frac{1}{2}\left(\frac{\partial v}{\partial x}\right)^2-\frac{\gamma(t)}{E}\right]=0, \tag{9}$$

$$m\frac{\partial^2 v}{\partial t^2}+c_d\frac{\partial v}{\partial t}+EI\frac{\partial^4 v}{\partial x^4}+\frac{\partial c}{\partial x}+\frac{\partial}{\partial x}\left[\left(\int_0^x p\,\mathrm{d}\xi\right)\frac{\partial v}{\partial x}\right]-EA\frac{\partial}{\partial x}\left\{\left[\frac{\partial u}{\partial x}+\frac{1}{2}\left(\frac{\partial v}{\partial x}\right)^2-\frac{\gamma(T)}{E}\right]\frac{\partial v}{\partial x}\right\}=0. \tag{10}$$

Eq. (9) will be satisfied assuming

$$\frac{\partial u}{\partial x}+\frac{1}{2}\left(\frac{\partial v}{\partial x}\right)^2-\frac{\gamma(T)}{E}=\text{constant}=\bar{\delta}(T), \tag{11}$$

where $\bar{\delta}(T)$ is equal to the average strain of the system, therefore

$$\bar{\delta}(T)=\frac{1}{L}\int_0^L\left[\frac{\partial u}{\partial x}+\frac{1}{2}\left(\frac{\partial v}{\partial x}\right)^2-\frac{\gamma(T)}{E}\right]\mathrm{d}x=\frac{1}{2L}\int_0^L\left(\frac{\partial v}{\partial x}\right)^2\mathrm{d}x-\frac{\gamma(T)}{E}. \tag{12}$$

Substituting Eq. (12) into Eq. (10), the equation of motion is derived as

$$m\frac{\partial^2 v}{\partial t^2}+c_d\frac{\partial v}{\partial t}+EI\frac{\partial^4 v}{\partial x^4}+\frac{\partial c}{\partial x}+\frac{\partial}{\partial x}\left[\left(\int_0^x p\,\mathrm{d}\xi\right)\frac{\partial v}{\partial x}\right]+\left[A\gamma(T)-\frac{EA}{2L}\int_0^L\left(\frac{\partial v}{\partial x}\right)^2\mathrm{d}x\right]\frac{\partial^2 v}{\partial x^2}=0. \tag{13}$$

2.3. Electromagnetic force **F** and torque **c**

As derived in Ref. [12], the electromagnetic force **F** and torque **c** acting on a volume V are

$$\mathbf{F}=\int\sigma(\dot{\mathbf{r}}\times\mathbf{B}_0)\times\mathbf{B}_0\mathrm{d}V, \tag{14}$$

$$c=\int\mathbf{M}\times\mathbf{B}_0\,\mathrm{d}V, \tag{15}$$

where σ is the conductivity of the material, $\mathbf{B_0}$ is the magnetic field, $\dot{\mathbf{r}}$ is the velocity of body motion, and $\mathbf{M}=\chi(\mu_0\mu_r)^{-1}\mathbf{B}$ is the volume density of magnetization in the body. μ_0 is the permeability of the vacuum, μ_r is the relative permeability, and $\chi=1-\mu_r$ is the susceptibility, and **B** is the magnetic induction vector.

3. Analytical procedure

3.1. Displacement function

In this study, the fist mode is considered and the displacement function can be written as

$$v(x,t)=w(t)\sin\lambda x,\quad 0\leqslant x\leqslant L, \tag{16}$$

where $\lambda=\pi/L$. An inextensible beam is assumed, and then

$$\int_0^x[1+v'^2(\xi,t)]^{1/2}\mathrm{d}\xi=s, \tag{17}$$

where s is the length of the beam from 0 to x. Differentiating Eq. (17) with respect to t, becomes

$$\int_0^x\left[\frac{v'\dot{v}'}{(1+v'^2)^{1/2}}\right]\mathrm{d}\xi+[1+v'^2]^{1/2}\dot{x}=0 \tag{18}$$

and the velocity in x-direction is

$$\dot{x} = \mathrm{d}x/\mathrm{d}t = -\frac{1}{(1+v'^2)^{1/2}}\int_0^x \frac{v'\dot{v}'}{(1+v'^2)^{1/2}}\,\mathrm{d}\xi. \tag{19}$$

Substituting Eq. (19) into Eq. (16), the velocity in x-direction becomes

$$\dot{x} = \dot{r}(x,w) = -\frac{\dot{w}}{2\lambda w[1+(2/\lambda^2 w^2)+\cos 2\lambda x]^{1/2}} \int_0^x \frac{1+\cos\xi}{[1+(2/\lambda^2 w^2)+\cos\xi]^{1/2}}\,\mathrm{d}\xi \tag{20}$$

and substituting it into Eq. (14) leads to the electromagnetic force as follows

$$\mathbf{F} = p\vec{i} = -(\sigma/2)hdB_m^2(1+\cos 2\Omega t)\dot{r}(x,w)\vec{i}. \tag{21}$$

The magnetization $\mathbf{M}$ can be derived using the same way as presented in Ref. [1], then the body couple can be obtained

$$\mathbf{c} = \int \mathbf{M}\times\mathbf{B}_0\mathrm{d}V = \lambda\Phi d\,\cos\lambda x(1+\cos 2\Omega t)w\vec{k}, \tag{22}$$

where $\Phi = \chi^2 B_m^2\sinh(\lambda h/2)/(\mu_0\mu_r\lambda\Delta)$ and $\Delta = \mu_r\,\sinh(\lambda h/2)+\cosh(\lambda h/2)$.

Substituting Eqs. (20)–(22) into Eq. (13) leads to a linear operator $\Pi(w)$

$$\Pi(w) = \left\{\left[m\ddot{w}+c_d\dot{w}-\lambda^2\Phi d(1+\cos 2\Omega t)w+EI\lambda^4 w+\frac{1}{4}EA\lambda^4 w^3-A\lambda^2\gamma(T)w\right]\sin\lambda x - \left(\frac{\sigma}{2}\right)hdB_m^2(1+\cos 2\Omega t)\left[\dot{r}(x,w)\lambda w\,\cos\lambda x-\lambda^2 w\,\sin\lambda x\int_0^x \dot{r}(x,w)\mathrm{d}x\right]\right. = 0. \tag{23}$$

3.2. Temperature effects

The conductivity σ of a material is reciprocal of its resistivity, so $\sigma = 1/\vartheta$, where ϑ is the resistivity of the material. In addition, the temperature and resistivity of material are dependent, since they are related by the relation

$$\vartheta = \vartheta_0 + \vartheta_0\alpha_r\Delta T, \tag{24}$$

where ϑ_0 is the resistivity at room temperature and α_r is temperature coefficient of resistivity. In this study, the thermal expansion is cancelled out by equal and opposite contraction caused by the restraining force, due to the total strain is zero at its ends. Once the nonlinear stress-temperature coefficient $\gamma(t)$ has been known, then the magnitude of the restraining force P_t can be obtained

$$P_t = -EA\alpha\Delta T - \hbar A\alpha^2\Delta T^2. \tag{25}$$

3.3. Galerkin's method

Taking $\sin\lambda x$ as the base function, Galerkin's equation leads to

$$\int_0^L \Pi(w)\sin\lambda x\,\mathrm{d}x = 0. \tag{26}$$

By, simplifying Eq. (26), a time-dependent differential equation is derived as follows:

$$w_{,tt}+2[\kappa+\zeta(1+\cos 2\Omega t)w^2]w_{,t}+(\omega_L^2-\xi\,\cos 2\Omega t)w+\eta w^3 = 0, \tag{27}$$

where ρ is density of the beam,

$$2\kappa = \frac{c_d}{\rho h d},$$

$$2\zeta = \frac{\sigma B_m^2 \lambda}{2\rho L} \frac{\int_0^L \dot{r}(x,w)\sin(2\lambda x)\mathrm{d}x - 2\lambda \int_0^L (\int_0^x \dot{r}(x,w)\mathrm{d}x)\sin^2 \lambda x \,\mathrm{d}x}{w_{,t} w},$$

$$\omega_0^2 = \frac{EI\lambda^4}{\rho h d}, \quad \omega_L^2 = \omega_0^2 \left(1 - \frac{B_r^2}{B_c^2} - \frac{EA\alpha\Delta T + \hbar A \alpha^2 \Delta T^2}{P_c}\right), \quad B_r^2 = \frac{B_m^2}{2},$$

$$B_c^2 = \frac{EI\lambda^3 \mu_0 \mu_r \Lambda}{2\chi^2 d \sinh(\lambda h/2)}, \quad P_c = EI\lambda^2 = EI\frac{\pi^2}{L^2},$$

$$\xi = \frac{b\lambda^2}{\rho h}, \quad \eta = \frac{E\lambda^4}{4\rho}, \quad \sigma = \frac{1}{\vartheta_0 + \vartheta_0 \alpha_r \Delta T}.$$

The ω_0 is the free transverse vibration natural frequency, ω_L is the transverse vibration of the beam subjected to transverse magnetic fields and thermal loads. In this study, the new parameter are defined as $\Omega = \varpi/\omega_L$, $\tau = \varpi t$, $k_1 = \kappa/\omega_L$, $k_2 = \zeta/\omega_L$, $2\varphi = \xi//\omega_L^2$, and $k_3 = \eta//\omega_L^2$. The frequency ratio Ω is also called the reduced natural frequency [14]. The Eq. (27) is simplified to well-known Mathieu equation.

$$\Omega^2 \frac{\mathrm{d}^2 w}{\mathrm{d}\tau^2} + 2\Omega[k_1 + k_2(1+\cos 2\tau)w^2]\frac{\mathrm{d}w}{\mathrm{d}\tau} + (1 - 2\varphi \cos 2\tau)w + k_3 w^3 = 0. \tag{28}$$

3.4. The IHB formulation

The procedure of the IHB method used to solve Eq. (28) is mainly divided into two steps that have been discussed in Refs. [13–15]. The first step is a Newton–Raphson procedure. The second step is to find an approximate solution by assuming a periodic solution and applying Galerkin's method.

The current state of vibration corresponding to a point (Ω_0, φ_0) on instability boundary is denoted by w_0. A neighboring state is reached through a parameter incrementation:

$$\varphi = \varphi_0 + \Delta\varphi, \quad \Omega = \Omega_0 + \Delta\Omega, \quad w = w_0 + \Delta w. \tag{29}$$

Substituting Eq. (29) into Eq. (28) and neglecting the nonlinear terms of $\Delta\varphi$, $\Delta\Omega$, Δw, a linearized incremental equation is obtained:

$$\begin{aligned}&\Omega_0^2 \Delta\ddot{w} + 2\Omega_0[k_1 + k_2(1+\cos 2\tau)w_0^2]\Delta\dot{w} + (1 - 2\varphi_0 \cos 2\tau)\Delta w \\ &\quad + 3k_3 w_0^2 \Delta w + 4\Omega_0 k_2 (1+\cos 2\tau) w_0 \Delta w \Delta\dot{w} \\ &\quad = R + 2\Delta\varphi w_0 \cos 2\tau - 2\Delta\Omega\Omega_0\ddot{w}_0 - 2\Delta\Omega[k_1 + k_2(1+\cos 2\tau)w_0^2]\dot{w}_0,\end{aligned} \tag{30a}$$

where

$$R = -\{\Omega_0^2 \ddot{w}_0 + 2\Omega_0[k_1 + k_2(1+\cos 2\tau)w_0^2]\dot{w}_0 + (1 - 2\varphi_0 \cos 2\tau)w_0 + k_3 w_0^3\}. \tag{30b}$$

The approximate functions w_0 and Δw can be expanded into a truncated Fourier series

$$w_0(\tau) = \sum_{k=1,3,\ldots}^{2N-1} (a_k \sin k\tau + b_k \cos k\tau) \quad \text{and} \quad \Delta w(\tau) = \sum_{k=1,3,\ldots}^{2N-1} (\Delta a_k \sin k\tau + \Delta b_k \cos k\tau) \tag{31}$$

for the principal region of instability, corresponding to a solution of period 2π. N is the number of temporal terms for calculation.

Substituting Eq. (31) into Eq. (30a) and using the Galerkin's procedure, a set of linear equations can be obtained as the following:

$$[C]\{\Delta a\} = \{R\} + \Delta\varphi\{P\} + \Delta\Omega\{Q\}, \tag{32}$$

where $[C]$ is the matrix for the Fourier coefficients and $\{\Delta a\}$ is a vector consisting of Fourier coefficients Δa_k or Δb_k, for example: $\{\Delta a\}^{\mathrm{T}} = \{\Delta a_1, \Delta a_3, \Delta a_5, \ldots\}$. $\{R\}$ is the corrective vector derived from Eq. (30b), and $\{P\}$, $\{Q\}$ are vectors obtained from the second and third right-hand side terms, respectively.

In Eq. (32), a linear system of $2N$ equations with $2N+2$ unknowns Δa, $\Delta\varphi$ and $\Delta\Omega$ has to be solved at each incremental step. Hence, it is necessary to add two constraints among Δa, $\Delta\varphi$ and $\Delta\Omega$. For example, the boundary curve in the (Ω, φ) plane, with $\|a\|$ as a parameter. The quantity $\|a\|$ has to be constant through the incremental steps, determining the first constraint to be: $\|a\| = \|a + \Delta a\|$. In this study, the Euclidian norm has been used to solve the problem:

$$||a|| = \left[\sum_{k=1,3,5\ldots}^{2N-1} (a_k^2 + b_k^2)\right]^{1/2}. \tag{33}$$

These choices and corresponding procedures used to solve Eq. (32) are discussed in Refs. [13–15].

4. Numerical results and discussions

A low-carbon steel is considered in this study, where the physical parameters of this system are given as $E = 1.94 \times 10^{11}\,\mathrm{Pa}$, $\rho = 7930\,\mathrm{kg/m^3}$, $L = 0.5\,\mathrm{m}$, $L/h = 85$, $d = 10^{-2}\,\mathrm{m}$, $\mu_r = 3.0 \times 10^3\,\mathrm{Hm^{-1}}$, $\alpha = 11 \times 10^{-6}\,^{\circ}\mathrm{C^{-1}}$, $\mu_0 = 1.26 \times 10^{-6}\,\mathrm{Hm^{-1}}$, $\alpha_r = 6.5 \times 10^{-3}\,^{\circ}\mathrm{C^{-1}}$, $\vartheta_0 = 9.68 \times 10^{-8}\,\Omega\mathrm{m}$ (ohm-meter), $\hbar/E = -140$.

When $c_d = 0$, $\Delta T = 0$ and the linear strain are considered, the principal region of dynamic instability of a simply supported beam-plate in an alternating magnetic field had been derived by Moon and Pao [1] and written as

$$\frac{\mathrm{d}^2 w}{\mathrm{d}t^2} + \omega_L^2(1 - 2\eta\cos 2\varpi t)w = 0, \tag{40}$$

where $\omega_L^2 = \omega_0^2(1 - B_r^2/B_c^2) = \omega_0^2(1 - \bar{B}^2)$, $2\eta = B_m^2/(2B_c^2 - B_m^2) = \bar{B}^2/(1 - \bar{B}^2)$, $\bar{B}^2 = B_m^2/2B_c^2 = B_r^2/B_c^2$, and ω_0^2 is defined the same as in Eq. (27). The results of instability in this study for a small deflection $\|a\| = 0.01$, and the results studied in Ref. [1] are shown in Fig. 2. In the present case, two solutions are found to be in good agreement.

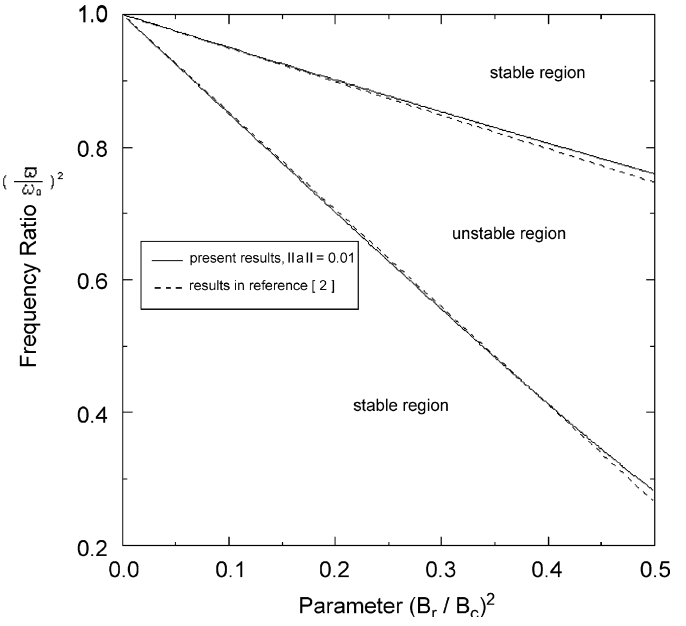

Fig. 2. The theoretical regions of instability of a simply supported beam-plate in a transverse magnetic field.

Using amplitude incrementation procedure as described in the previous section, the nonlinear effects of amplitudes on the principal instability region for the damping parameter $k_1 = 0$ and 0.1 in the (Ω, φ)-plane are shown in Fig. 3. It has been known that when viscous damping is included, then a least load factor φ is required to make a parameter vibration occur and it is varied with the amplitude. As can be seen in Fig. 3, when viscous damping is included, the boundary curves no longer consist of two different branches, but one single branch with a U-turn portion. Furthermore, the higher value of the amplitude $\|a\|$ is considered, the higher value of the frequency ratio Ω is obtained. Using the φ-incrementation procedure, the nonlinear effects of amplitude on the principal instability region in the $(\Omega, \|a\|)$-plane are shown in Fig. 4. For a fixed load factor, it appears that a smaller region of the principal instability is obtained by considering the higher value of amplitude $\|a\|$ given by Eq. (33). Fig. 5 shows the nonlinear influences of the amplitude on the frequency ratio for a fixed load factor $\varphi = 0.5$ and for different damping coefficients. The results show that when the damping coefficient k_1 is greater than 0.05, the branches curves become one close path, and an increase in damping parameter results in a reduction of the region of instability. One may note that, when damping coefficient is different from zero, the curves no longer consist of two distinct branches, but of one closed path. Because the value of frequency ratio Ω up to 3.0 is considered in this case, the turning point for $k_1 = 0.05$ lies outside of the highest limit of the horizontal axis used in Fig. 5. If the higher value of frequency ratio Ω is considered in this case, the boundary curve for $k_1 = 0.05$ will be one closed path.

To analyse the effects of varying the conditions of temperature increases, one considers $\|a\| = 0.5$, then $k_1 = 0$ and 0.1 are considered, respectively. The effects of increased temperature ΔT on the principal instability region are shown in Fig. 6, in which the regions of instability are shifted up with an increase in temperature, while $(B_r^2/B_c^2) + (EA\alpha\Delta T/P_{cr}) < 1$. In the current work, the temperature increase ΔT in the instability analysis is related to the fundamental natural frequency of the system and the conductivity of the material through the relations $\omega_L^2 = \omega_o^2 \times (1 - EA\alpha\Delta T/P_c)$ and $\sigma = 1/(\vartheta_0 + \vartheta_0\alpha_r\Delta T)$, respectively. In particular, the damping coefficient k_2 no longer is considered as the original value when the temperature increase is different from zero. Moreover, though the value of increased temperature is quite small in this study, the instability region changes obviously. Fig. 7 shows the nonlinear influences of amplitude on the frequency ratio for a fixed load factor $\varphi = 0.5$ with the different temperature increases. The results clearly show that the relative value of frequency ratio Ω becomes higher and the region of instability becomes smaller when the temperature increases, i.e. the increasing temperature increases the effect of nonlinear on the system.

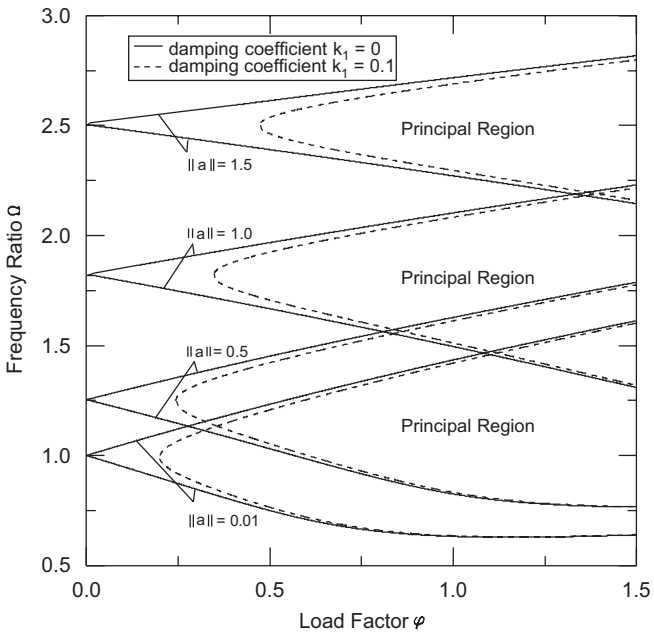

Fig. 3. The nonlinear effects of amplitude on the principal instability region for the damping parameter $k_1 = 0$ and 0.1.

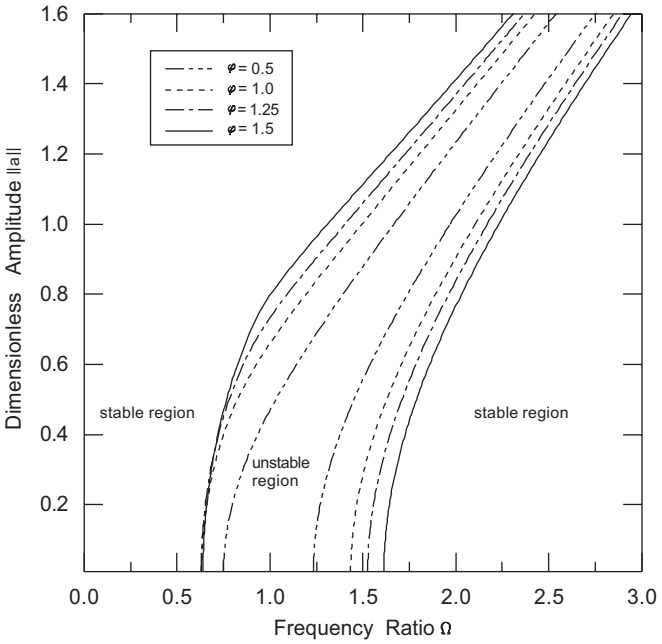

Fig. 4. The nonlinear effects of amplitude on the principal instability region for various load factors.

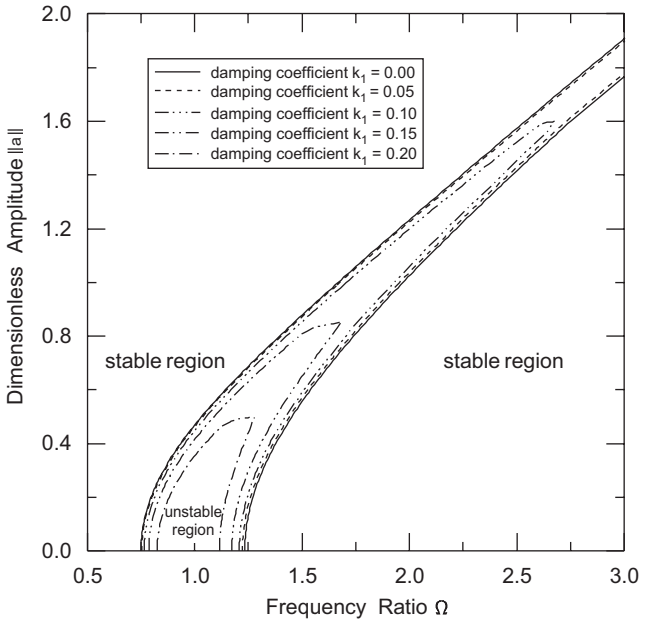

Fig. 5. The nonlinear influences of the amplitude on the frequency ratio for a fixed load factor $\varphi = 0.5$ with different damping coefficients.

5. Conclusions

Based on the magneto-solids mechanics and the large deformation, the theoretical model has been obtained for a pinned beam subjected to an alternating magnetic field and thermal load. Through the principal of

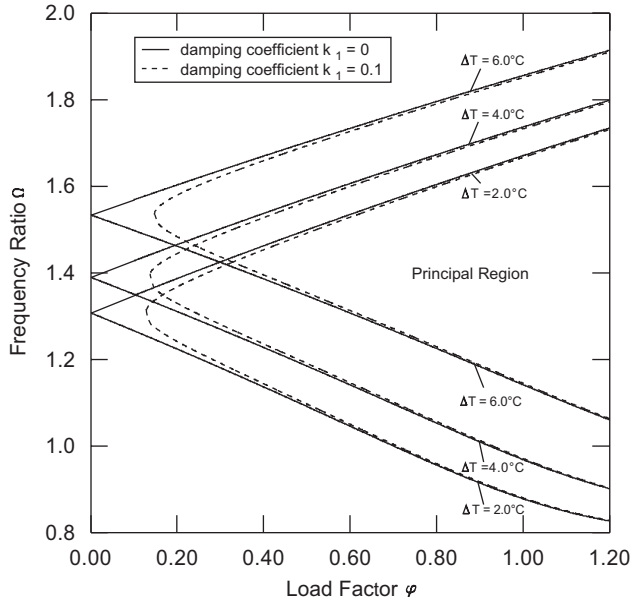

Fig. 6. The effects of increased temperature ΔT on the principal instability region for $\|a\| = 0.5$.

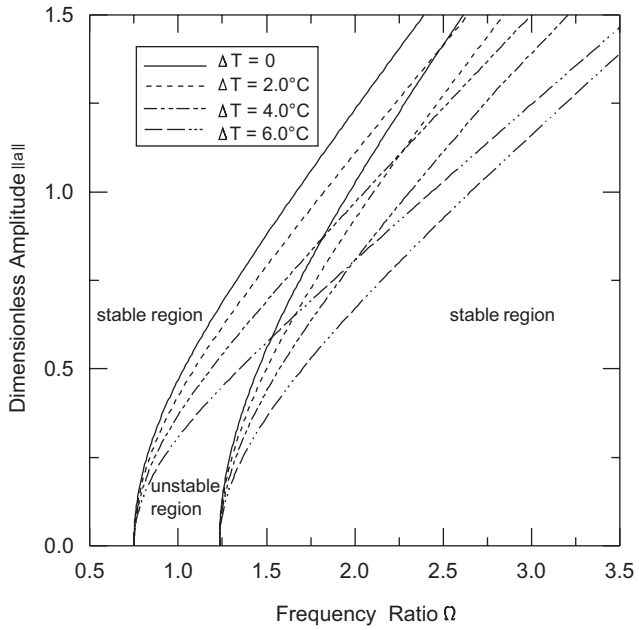

Fig. 7. The nonlinear influences of amplitude on the frequency ratio for a fixed load factor $\varphi = 0.5$ with the different increased temperatures.

minimum of potential energy and the Galerkin's method, the nonlinear governing equation is derived. In this case, the model is symmetric with respect to the mid-surface of the beam and the magnetic field is spatially uniform, the body force **F** and body couple **c** on the beam can be simplified and led to a nonlinear damping effect. By using the IHB method, the principal instability regions have been shown in the parameter space of the excitation parameterφ versus frequency ratio Ω, the frequency ratio Ω versus dimensionless amplitude $\|a\|$,

and the effect of thermal loads on the region of instability. The results show that the region of instability is sensitivity dependent upon the amplitude $\|a\|$, the excitation φ, the increased temperature ΔT and the damping parameter k_1. Considered as a small deflection of a beam-plate in an oscillating magnetic filed only, the results of instability carried out by the IHB method agreed well with the results of Moon and Pao [2].

In should be noted that each buckling mode has its own safe temperature increase and magnetic field increase. Under the value of buckling, increasing either the transverse magnetic field or the thermal load leads to a decreasing fundamental natural frequency. Though the value of temperature increase is small for slender sections in this study, the effect of thermal load on the instability region is obvious. Moreover, either the higher temperature increase or the higher value of amplitude $\|a\|$ is considered, the higher value of frequency ratio Ω is obtained. It is believed that the increasing temperature increases the effect of nonlinear on the system. This is for an increase in the temperature, the fundamental natural frequency and conductivity of the material will always coincide with the relations of $\omega_L^2 = \omega_0^2 \times [1 - (EA\alpha\Delta T + \hbar A\alpha^2\Delta T^2)/P_c]$ and $\sigma = 1/(\vartheta_0 + \vartheta_0\alpha_r\Delta T)$.

References

[1] F.C. Moon, Y.H. Pao, Magnetoelastic buckling of a thin plate, *ASME Journal of Applied Mechanics* 35 (1968) 53–58.

[2] F.C. Moon, Y.H. Pao, *Vibration and dynamic instability of a beam-plate in a transverse magnetic field* 36 (1969) 92–100.

[3] K. Miya, T. Takagi, Y. Ando, Finite element analysis of magnetoelastic buckling of a ferromagnetic beam-plate, *ASME Journal of Applied Mechanics* 47 (1980) 377–382.

[4] A.C. Eringen, Theory of electromagnetic elastic plates, *International Journal of Engineering Science* 27 (1989) 363–375.

[5] J.S. Lee, Destabilizing effect of magnetic damping in plate strip, *ASCE Journal of Engineering Mechanics* 118 (1992) 161–173.

[6] T. Tagaki, J. Tani, Y. Matsubara, T. Mogi, Dynamic behavior of fusion structural components under strong magnetic fields, *Fusion Engineering and Design* 27 (1995) 481–489.

[7] Y.S. Shih, G.Y. Wu, J.S. Chen, Transient vibrations of a simply-supported beam with axial loads and transverse magnetic fields, *Mechanics of Structures and Machines* 26 (1998) 115–130.

[8] Y.H. Zhou, Y.W. Gao, X.J. Zheng, Q. Jiang, Buckling and post-buckling of a ferromagnetic beam-plate induced by magnetoelastic interactions, *International Journal of Non-linear Mechanics* 35 (2000) 1059–1065.

[9] X.J. Zheng, X.Z. Wang, Analysis of magnetoelastic interaction of rectangular ferromagnetic plates with nonlinear magnetization, *International Solids and Structures* 38 (2001) 8641–8865.

[10] E.A. Thorton, *Thermal Structures for Aerospace Applications*, AIAA Education Series, Reston, VA, 1996.

[11] P. Ribeiro, E. Manoach, The effect of temperature on the large amplitude vibrations of curved beams, *Journal of Sound and Vibration* 285 (2005) 1093–1107.

[12] G.Y. Wu, The analysis of dynamic instability and vibration motions of a pinned beam with transverse magnetic field and thermal loads, *Journal of Sound and Vibration* 284 (2005) 343–360.

[13] S.L. Lau, Y.K. Cheung, Amplitude incremental variational principle for nonlinear vibration of elastic systems, *ASME Journal of Applied Mechanics* 48 (1981) 959–964.

[14] S.L. Lau, Y.K. Cheung, S.Y. Wu, A variable parameter incrementation method for dynamic instability of linear and nonlinear systems, *ASME Journal of Applied Mechanics* 49 (1982) 849–853.

[15] S.L. Lau, S.W. Yuen, Solution diagram of non-linear dynamic systems by the IHB method, *Journal of Sound and Vibration* 167 (1993) 303–316.

[16] F. Ziegler, G. Rammerstorfer, Thermoelastic Stability, in: R.B. Hetnarski (Ed.), *Thermal Stress*, Vol. III, Elsevier, Amsterdam, 1989.

[17] T. Jekot, Nonlinear problems of thermal postbuckling of a beam, *Journal of Thermal Stresses* 19 (1996) 359–367.